HHS Public Access

Author manuscript

Exp Eye Res. Author manuscript; available in PMC 2016 August 30.

Published in final edited form as:

Exp Eye Res. 2016 May ; 146: 341–353. doi:10.1016/j.exer.2016.04.006.

ASSESSMENT OF VISUAL FUNCTION AND RETINAL STRUCTURE FOLLOWING ACUTE LIGHT EXPOSURE IN THE LIGHT SENSITIVE T4R RHODOPSIN MUTANT DOG

Simone Iwabe[a], **Gui-Shuang Ying**[b], **Gustavo D. Aguirre**[a], and **William A. Beltran**[a,1]

[a]Section of Ophthalmology, School of Veterinary Medicine, University of Pennsylvania, Philadelphia, Pennsylvania 19104 USA

[b]Scheie Eye Institute, Department of Ophthalmology, University of Pennsylvania Perelman School of Medicine, Philadelphia, Pennsylvania 19104 USA

Abstract

The effect of acute exposure to various intensities of white light on visual behavior and retinal structure was evaluated in the T4R *RHO* dog, a naturally-occurring model of autosomal dominant retinitis pigmentosa due to a mutation in the Rhodopsin gene. A total of 14 dogs (ages: 4–5.5 months) were used in this study: 3 homozygous mutant $RHO^{T4R/T4R}$, 8 heterozygous mutant $RHO^{T4R/+}$, and 3 normal wild-type (WT) dogs. Following overnight dark adaptation, the left eyes were acutely exposed to bright white light with a monocular Ganzfeld dome, while the contralateral right eye was shielded. Each of the 3 homozygous ($RHO^{T4R/T4R}$) mutant dogs had a single unilateral light exposure (LE) to a different (low, moderate, and high) dose of white light (corneal irradiance/illuminance: 0.1 mW/cm^2, 170 lux; 0.5 mW/cm^2, 820 lux; or 1 mW/cm^2, 1590 lux) for 1min. All 8 heterozygous ($RHO^{T4R/+}$) mutant dogs were exposed once to the same moderate dose of light. The 3 WT dogs had their left eyes exposed 1, 2, or 3 times to the same highest dose of light. Visual function prior to LE and at 2 weeks and 33 weeks after exposure was objectively assessed in the $RHO^{T4R/T4R}$ and WT dogs by using an obstacle-avoidance course. Transit time through the obstacle course was measured under different scotopic to photopic ambient illuminations. Morphological retinal changes were evaluated by non-invasive *in vivo* cSLO/sdOCT imaging and histology before and at several time-points (2–36 weeks) after light exposure. The analysis of the transit time through the obstacle course showed that no differences were observed in any of mutant or WT dogs at 2 weeks and 33 weeks post LE. The $RHO^{T4R/T4R}$ retina exposed to the lowest dose of white light showed no obvious changes in ONL thickness at 2 weeks, but mild decrease was noted 36 weeks after LE. The $RHO^{T4R/T4R}$ retina that received a moderate dose (showed an obvious decrease in ONL thickness along the superior and temporal meridians at 2 weeks post LE with more severe damage at 36 weeks post LE in all four meridians. The $RHO^{T4R/T4R}$ retina exposed to the high dose showed at 2 weeks after LE extensive ONL damage in all four meridians. This light intensity did not cause any retinal damage in WT dogs even after repeated (up to 3) LE. Analysis of ONL thickness in heterozygous mutant dogs exposed to the moderate dose of light confirmed the increased sensitivity to light damage of the superior/tapetal retina, and the occurrence of an ongoing cell death process several weeks after the acute

[1]To whom correspondence should be addressed. wbeltran@vet.upenn.edu.

LE. In conclusion, a short single exposure to a dose of white light that is not retinotoxic in WT dogs causes in the T4R *RHO* retina an acute loss of ONL in the central to mid peripheral region that keeps progressing over the course of several weeks. However, this severe retinal damage does not affect visual behavior presumably because of islands of surviving photoreceptors found in the *area centralis* including the newly discovered canine fovea-like area, and the lack of damage to peripheral photoreceptors.

Keywords

Rhodopsin; ADRP; light damage; retinal degeneration; vision; canine model

1. Introduction

Retinitis pigmentosa (RP) is a genetically heterogenous group of retinal degenerations with a prevalence of approximately 1 in 4,500.(1, 2) Most familial cases are inherited as X-linked, autosomal dominant or recessive. Autosomal dominant RP (ADRP) accounts for 30–40% of all RP cases,(3) and, among the 18 causative genes identified to this date (http://www.sph.uth.tmc.edu/Retnet/), mutations in the rhodopsin gene (*RHO*) are responsible for up to 30% of cases.(4–9)

Human patients affected with *RHO*-ADRP typically show either a diffuse rod-cone dystrophy or a regional disease that affects primarily the inferior retina.(10) A functional classification proposed by Cideciyan et al.(11) defines two major phenotypes that comprise class A mutants with a retina-wide severe loss of rod function early in life, and class B mutants for which rod sensitivity loss occurs in adulthood. Among class B mutants is a subgroup termed class B1 that shows a gradient of dysfunction with more severe rod sensitivity loss in the nasal and pericentral retina, and less impairment in the supero-temporal quadrant. Exposure to high levels of environmental light originating from above has been suggested to exacerbate the course of rod loss in these patients and contribute to these altitudinal visual field defects.(12) In support of this hypothesis are a limited number of case reports of *RHO*-ADRP patients with an occupational history of exposure to bright illumination and the occurrence of sectoral/altitudinal disease.(13, 14) Furthermore, vulnerability to light has been demonstrated in several animal models of *RHO*-ADRP including: transgenic *X. laevis* expressing human P23H, T4K, T17M, N2S/N15S *RHO* mutations; (15–17) mice with P23H, (18) T17M, (19, 20) Y102H, (21) I307N (21) mutations; the P23H, (22–24) and S334ter (23) rats; and the T4R dog (25). Within this group of animal models, there is a spectrum of sensitivity to light, with, at one extreme, the T17M *RHO* mouse and the T4R *RHO* dog. Such observations have raised significant concern that even short periods of exposure to light levels such as those typically used in clinical ophthalmology procedures may accelerate the course of rod photoreceptor cell death in Class B1 patients.(25)

Mutations in *RHO* are one of the most common molecularly identified causes of inherited retinal degeneration, yet, in spite of an increasing understanding of the diversity and complexity of the pathogenic mechanisms that link specific mutations to the death of rods

(26) that could be targeted, (27) this has not yet translated into the development of novel therapeutics. A different approach is the use of corrective gene therapy. While some *RHO* mutations have been suggested to produce a dominant negative effect (28, 29) and thus may be approached via a gene replacement strategy, (30) the majority of *RHO* mutations are thought to cause disease through gain-of-function mechanisms, although possible dominant-negative mechanisms have been proposed.(26) This, coupled with allelic heterogeneity has led several groups to consider a mutation-independent approach in which both mutant and wild-type *RHO* mRNAs are suppressed and replaced with a resistant (hardened) wild-type gene.(31, 32)

There is now ample evidence for the value of using large animal models of inherited retinal degenerations to assess the efficacy and pre-clinical safety of retinal gene therapies.(33–37) In the context of *RHO*-ADRP, the T4R *RHO* dog (38) offers the ability to experimentally trigger via light exposure the onset of retinal degeneration, and rapidly assess the efficacy of therapeutic intervention. A preliminary requirement before initiating such studies is to establish outcome measures of structural and functional retinal integrity that could be used to test whether corrective gene therapy is effective. To this end, the present study correlates light exposure doses to the canine T4R *RHO* retina with the extent of photoreceptor loss and alterations in visually-guided behavior.

2. Materials and Methods

2.1 Animals

Three $RHO^{T4R/T4R}$ dogs (age: 4 months, 2 males and 1 female), eight $RHO^{T4R/+}$ dogs (age: 5–5.5 months, 6 males, 2 females) and 3 wildtype (WT) dogs (age: 4–5 months, 3 females) were used in this study. Dogs were housed at the Retinal Disease Studies facility (Kennett Square, Pennsylvania), and kept under standard kennel light illuminations since birth (cycles of 12 hours of light ~175–350 lux at the level of the “standard” dog eye and 12 hours of dark environment).. This study was conducted in accordance with the ARVO resolution on the Use of Animals in Ophthalmic and Vision Research and the University of Pennsylvania Institutional Animal Care and Use Committee.

To familiarize the dogs with the investigators and the testing conditions, the animals were allowed to play in the testing room under dim illumination (0.2 lux) for 30 to 45 minutes, three to four times a week for a period of 2 to 4 weeks. During this socialization period the dogs were gradually trained to wear an opaque ocular shield in one eye (Oculo-Plastik, Inc., Montreal, Quebec, Canada); and to respond to voice commands and rewards such as vocal praise, toys and treats. During this time all dogs were trained in a 3.6 meter-long obstacle – avoidance course (38) without any of the obstacle panels inserted. Once the dogs were comfortable with their surroundings, panels were added to the visual testing apparatus, and their training completed.

2.2 Light exposure (LE)

Dogs were dark-adapted overnight, and on the morning of the procedure their pupils were dilated with 1% tropicamide and 1% phenylephrine, 3 times, 30 minutes apart in both eyes.

Dogs were anesthetized with Ketamine (10 mg/Kg) and Diazepam (0.5 mg/Kg) IV. To prevent the ventral rotation induced by the general anesthesia a retrobulbar saline injection (5–10 ml) was performed to recenter the eyes in the primary gaze position. Left eyes were exposed to different light intensities (see below) and right eyes were completely shielded from light with the opaque ocular shield. The left eye was exposed for 1 min to constant white light (6500 K) using a monocular Ganzfeld dome from the Espion electrophysiology system (ColorBurst; Diagnosys LLC, Lowell, MA, USA). Animals were maintained under dim red illumination prior to, during, and up to 24 hours after the procedure, which allowed the pupils to return to their physiological resting position before they were returned to the cyclic light environment of the kennels.

Each of the 3 homozygous mutant (*RHO*$^{T4R/T4R}$) dogs had its left eye light exposed for 1 minute, but to a different dose of white light: 0.1 mW/cm^2, hereafter termed “low dose” (T4R #1), 0.5 mW/cm^2 termed “moderate dose” (T4R #2), or 1 mW/cm^2 termed “high dose” (T4R #3). The high dose (1mW/cm^2 for 1 min) is known to cause acute and severe retinal degeneration in T4R RHO dogs.(39) Corneal irradiances were measured with the radiometric function of a light meter (IL1700, International Light Technologies Inc, Newburyport, MA, USA) placed at the entrance of the monocular Ganzfeld. Light intensities measured in lux units with the photometer function provided the following equivalent illuminance values: 170 lux (low dose), 820 lux (moderate dose) and 1590 lux (high dose). Thirty-four weeks after the first light exposure, each of the 3 *RHO*$^{T4R/T4R}$ dogs had its previously shielded right eye exposed to the same light intensity used to expose the left eye. During this second exposure, the left eye was occluded (see SI Fig S1A). To verify that the light intensities used to cause retinal damage in the *RHO*$^{T4R/T4R}$ retina is not toxic to the WT retina, 3 normal dogs were exposed to the same “high dose” of light (corneal irradiance of 1 mW/cm^2 for 1 min; 1590 lux); however, dog N#1 had the left eye exposed once, dog N#2 was exposed twice and dog N#3 was exposed 3 times with a 3 week interval between exposures (see SI Fig.S1B). As the dose-response study was conducted in a limited number (n=3) of RHO$^{T4R/T4R}$ dogs, we subsequently decided to test the effect of the moderate dose of light (0.5 mW/cm^2 for 1 min; 820 lux) in a higher number of heterozygous mutant (RHO$^{T4R/+}$) animals (see SI Fig.S1C). Using a similar approach as for the RHO$^{T4R/T4R}$ (n= 3; right eyes), and WT (n =1; left eye) dogs, the effect of light was assessed at the same 2 week post LE time-point in a group of 4 RHO$^{T4R/+}$ dogs. Another group of 4 dogs was assessed at 6 weeks post LE to examine the occurrence of continuing retinal degeneration between 2 and 6 weeks post LE.

2.3 Visual behavior test

An obstacle-avoidance course was used in this study as previously described.(40) The 3.6 meter-long obstacle course included 5 panels that could be moved either to the left or to the right side. The panel positions were changed between runs to prevent the dogs from memorizing the position of the obstacle panels. Specific obstacle panel combinations were randomly arranged and all dogs were tested with the same obstacle panel combinations. A digital camera (Sony Handycam) was attached above the testing apparatus to a moveable platform to follow the dogs navigating through the course. The infrared imaging function of the camera enabled recording under the dimmest light conditions.

One tungsten halogen stage light (Tota-light, Lowel Light Inc, Brooklyn, NY) with a dimmer was mounted on 1.8 m tall tripod and set halfway through the length of the course. Four different ambient illuminations that ranged from mesopic to photopic conditions (0.2; 1; 10; and 65 lux) measured with the IL1700 light meter at a dog's eyes level were set within the course by dimming the brightness of the tungsten halogen and turning ON or OFF the overhead fluorescent lights in the testing room. Three additional lower ambient illuminations (0.003; 0.009; and 0.03 lux) were subsequently used in the second arm of the study to test the dogs under scotopic conditions. This was achieved by using two incandescent lamps (helical 15w 120vac 60Hz 190mA) with polarized filters. One lamp was placed at the beginning and one at the end of the course.

The visual behavior experiments were carried out indoors under the artificial light conditions described above. Homozygous mutant (*RHO*$^{T4R/T4R}$) dogs underwent first a light exposure of their left eye and 34 weeks later of their right eye was exposed as described below and summarized in SI Fig.S1A.

Visual behavior in the obstacle avoidance course was assessed 1 week before and 2 weeks after LE in the left eye under mesopic/photopic illuminations (0.2; 1; 10; and 65 lux), and then at 33 weeks post exposure under scotopic/mesopic illuminations (0.003; 0.009; 0.03; and 0.2 lux). To complete the analysis of visual behavior under scotopic/mesopic illuminations (0.003; 0.009; 0.03; and 0.2 lux), each *RHO*$^{T4R/T4R}$ dog had subsequently its right eye light-exposed and its visually-guided behavior tested 2 weeks later. Transit times from RHO$^{T4R/T4R}$ were compared to that of previously published WT dogs.(37) Transit time values from the right eyes obtained 1 week earlier were used as pre-light exposure values. Normal dogs were tested under mesopic/photopic illuminations before and 2 weeks after light exposure of their left eye (SI Fig S1B).

On the day of the test, the dogs were brought into the testing room and adapted for 20 minutes under the lowest intensity of ambient illumination that they were subsequently going to be tested. A total of 6 trials (3 trials/eye/illumination level) were performed with each dog before changing to the next light intensity level. The 6 trials were divided in two sets. In the first set of 3 trials the dogs ran the obstacle course with the same eye occluded but a different panel combination for each trial. In the second set of 3 trials, the dog was tested with the other eye occluded using the same three panel combinations as for the contralateral eye. At the end of every 3 trials an edible treat was given to encourage the dog to perform the next set of runs. After all dogs performed the 6 trials, the illumination was increased to the next level of brightness, and the obstacle course panel positions changed according to the predetermined scheme. Animals were light adapted for 10 minutes before being placed at the entrance for the next set of runs.

2.4 Non-invasive retinal imaging

In vivo retinal imaging was performed with dogs under general anesthesia using a combined confocal scanning laser ophthalmoscope (cSLO) and spectral-domain optical coherence tomography (sdOCT) Spectralis™ HRA/OCT device (Heidelberg Engineering, Germany). Morphological retinal changes were evaluated before, and 2 weeks after each light exposure in normal dogs. The left retinas from the *RHO*$^{T4R/T4R}$ mutant dogs were imaged 48 hrs

before, 2 weeks, 32 weeks and 36 weeks after the single light exposure of the left eyes (see Fig.S1), and the right retinas were imaged 2 weeks before and 2 weeks after a single light exposure of the right eyes

Near-infrared *en face* images from the fundus were acquired using a 55° lens and an 820 nm wave-length laser. Vertical and horizontal sdOCT raster scans were obtained using a 30° lens. All four central quadrants (superior, inferior, nasal and temporal) were scanned with the following settings: 30 ° x 20 ° scanned area with 49 sequential B-scans separated by a 120 μm distance and an average of 9 ART per scan. Single B-scans (100 ART) beginning at the optic nerve head (ONH) and extending along the 4 meridians (superior, inferior, nasal, temporal) were acquired and subsequently used to measure the ONL thickness (see Fig.S2). Raster and single scans were acquired using the high resolution mode. Segmentation of the ONL was done manually using the Heidelberg Eye Explorer program and the ONL thickness was measured every 1.76 degree along the 4 meridians. ONL segmentation of the temporal meridian was performed on an OCT scan acquired within the tapetal region, while for the nasal meridian it was selected from a scan acquired within the non-tapetal area (see SI Fig.S2). Using the device's automatic eye tracking system, all images acquired during the first examination were used as reference images for subsequent follow-up examinations, thus allowing longitudinal evaluation of changes in the same area.

2.5 Tissue processing, histopathology and immunohistochemistry (IHC)

At termination, eyes were collected under dim-red illumination while the dogs were maintained under general anesthesia with intravenous pentobarbital sodium. Following enucleation, the animals were immediately euthanatized with a pentobarbital overdose injected intravenously. The globes of the 3 homozygous mutant ($RHO^{T4R/T4R}$) and WT dogs were fixed in 4% paraformaldehyde (PFA) in 0.1M phosphate-buffered saline at 4°C after a slit was made with a razor blade anterior to the ora serrata. After 3 hours in 4% PFA, the posterior segment was isolated, the vitreous gently removed, and the eye cup fixed for an additional 24 hours in 2% PFA at 4°C. The tissues were trimmed to correspond to the areas scanned by OCT, and cryoprotected for 24 hours each in 15% and 30% sucrose in 0.1M sodium phosphate and 0.15M sodium chloride at 4°C. Tissues were then embedded in optimal cutting temperature medium, frozen, and stored at −80°C.

Ten μm-thick retinal cryosections extending along the superior, inferior, temporal and nasal meridians of both light exposed and shielded eyes from WT and $RHO^{T4R/T4R}$ dogs were cut and used for standard histological (H&E) staining and immunohistochemistry (IHC), as previously reported.(41) Rows of nuclei in the ONL were counted on standard H&E stained sections every 1,000 μm from the edge of the optic nerve head to the ora serrata. The section from the temporal meridian was within the tapetal region; while the nasal meridian section was obtained within the non-tapetal area (see SI Fig.S2). *In vivo* OCT B-scans and histological sections from approximately the same area were analyzed. Double fluorescence IHC using primary antibodies directed against rod opsin, human cone arrestin and RPE65 (Table 1) was performed as previously described (41) to identify the presence of remaining photoreceptors and RPE cells.

In the case of the 8 heterozygous ($RHO^{T4R/+}$) dogs, their eyes were fixed in Bouin's solution and paraffin-embedded to achieve optimal morphological preservation. Sagittal sections of the entire globe that included both the tapetal and non-tapetal fundus were cut, and H&E stained. Rows of nuclei in the ONL were counted every 1,000 μm from the edge of the optic nerve head to the ora serrata along both the superior and inferior meridians.

2.6 Statistical analysis

Assessment of visual behavior was done by measuring transit times from the first forward motion at the entrance of the obstacle course until the dog had completely exited it. These transit times were obtained from videos recorded during the test. In WT dogs, comparisons of transit time in the light exposed eye versus the shielded eye were done by using the analysis of variance. The correlations from repeated measures at different ambient illuminations and inter-eye correlations were accounted for by using the generalized estimating equation.(42) Due to the small sample size no formal statistical analysis was performed on the results from $RHO^{T4R/T4R}$ dogs. Instead, transit time results for each of the $RHO^{T4R/T4R}$ dogs were presented with descriptive statistics (Mean ± SD), and compared to the range of normal transit time values of WT dogs. In addition, based on prior experience with this same obstacle course to test dogs affected with either cone or rod visual impairment,(37, 40) we considered a transit time of ≤ 10 seconds to be normal.

Similarly, the mean ONL thickness at defined retinal locations from the ONH were plotted on spider graphs for each of the three homozygous mutant ($RHO^{T4R/T4R}$) dogs. In the case of the 2 groups of 4 heterozygous ($RHO^{T4R/+}$) a 1-tailed paired Student's t test was used to compare the mean ONL thickness in the shielded (right) eye, to that of the contralateral (left) light exposed eye. A 1-tailed $p < 0.05$ was considered as statistically significant.

3. Results

3.1 Light exposure does not alter visual performance of $RHO^{T4R/T4R}$ dogs

$RHO^{T4R/T4R}$ mutant dogs were analyzed individually. Transit times before light exposure from all 3 mutant dogs that ran under the same mesopic-low photopic ambient illumination conditions were comparable to transit times from normal dogs (Fig. 1 A).(37) At 2 weeks after LE, dogs that had been exposed to low and moderate doses of light did not show any differences in transit times between the left and right eye. The dog that received a high dose of light showed a 0.5 and 1 fold increase in transit time, respectively, under 1 and 10 lux of ambient illumination; however values from the exposed eye were within or close to the 95% CI of WT dogs In addition, no obvious differences were seen between the shielded and exposed eyes under other conditions of illumination (Fig 1 B). This unexpected lack of visual impairment lead us to retest all 3 $RHO^{T4R/T4R}$ dogs at 33 weeks post LE with a specific emphasis on analyzing rod-mediated behavior. Thus, at this time-point, dogs were run under scotopic/mesopic ambient illumination (0.003; 0.009; 0.03 and 0.2 lux). No differences in transit time were observed between shielded and exposed eyes in any of the three dogs (Fig. 1 C).

As visual behavior of the *RHO*$^{T4R/T4R}$ dogs was initially tested only under mesopic/photopic conditions at 2 weeks after LE, the experiment was extended to test the dogs under scotopic/mesopic illumination also at 2 weeks post LE. For this, the previously shielded right eye was exposed to the same light intensities as had been used for the left eye, and transit time measured under 0.003; 0.009; 0.03 and 0.2 lux. No differences in transit time were observed in any of the 3 *RHO*$^{T4R/T4R}$ dogs (Fig. 2).

Following acute bright light exposure (1590 lux), the 3 WT dogs were run under mesopic/photopic ambient illuminations conditions (0.2; 1; 10; and 65 lux). No statistically significant differences in transit times (Left eye: 4.50 ± 0.12 sec vs right eye: 4.47 ± 0.11 sec; $p = 0.84$) were noted between light exposed (left) and shielded (right) eyes at the 2 week time-point (Fig. 3).

3.2 Light-induced photoreceptor loss in T4R RHO is dose-dependent

Retinal imaging by cSLO/sd-OCT was performed along the superior, inferior, temporal and nasal meridians. There was no change in retinal vasculature in the *RHO*$^{T4R/T4R}$ mutant retina exposed to the low dose at 2 or 36 weeks after LE (Fig. 4 A_1, B_1, C_1). However, moderate exposure showed vascular attenuation as early as 2 weeks after LE (Fig. 4 D_1, E_1) that progressed and was more prominent at 36 weeks after LE (Fig. 4 F_1). This change was more pronounced in the high dose LE retina as early as 2 weeks after exposure (Fig. 4 G_1, H_1, I_1). Normal dogs did not show any observable abnormalities by cSLO after 1, 2 or 3 exposures to the high dose of light (Fig. 4 J_1, K_1, L_1, M_1). The vascular attenuation observed in the eyes exposed to the moderate and high dose light levels is illustrated in SI Fig S3.

SdOCT scans from the *RHO*$^{T4R/T4R}$ retina exposed to the low dose of light showed no obvious changes in ONL thickness in all 4 meridians at 2 weeks after LE (Fig. 4 A_2, B_2), nor in the temporal quadrant at 36 weeks after LE (Fig.4 C_2), yet, mild thinning at that time-point was detectable in the 3 remaining quadrants. Following moderate and high LE ONL thinning was detectable as early as 2 weeks after LE (Fig. 4 D_2, E_2, G_2, H_2), and was even more severe at 36 weeks after exposure. At this later time point, a thin ONL was still visible in the retina exposed to the moderate dose (Fig. 4 F_2). However, no ONL was detectable in the retina exposed to the high dose (Fig. 4 I_2). At this later time point a thinning of the inner retina (IPL, GCL, and NFL) was observed in the mutant retina exposed to the high dose of light (Fig. 4 I_2). Normal dogs did not show any noticeable change in ONL thickness after 1, 2 or 3 high dose exposures (Fig. 4 J_2, K_2, L_2, M_2).

Analysis of OCT raster scans performed along the 3 other meridians from *RHO*$^{T4R/T4R}$ retinas exposed to the low and high doses showed a similar thinning in retinal vasculature and ONL thickness as in the temporal meridian. While in retinas exposed to the moderate dose of light the superior and temporal meridians presented a similar ONL loss that was more severe than that observed in the nasal and inferior meridians (data not shown).

3.3 Acute light exposure causes rapid and progressive ONL thinning in the mutant T4R RHO retina

ONL thickness measurements from *RHO*$^{T4R/T4R}$ and normal retinas were performed on sdOCT B-scans by manual segmentation along the 4 meridians and up to 30° eccentricity

from the edge of the ONH. The *RHO*$^{T4R/T4R}$ mutant left retina exposed to the low dose showed limited to no decrease in ONL thickness 2 weeks after LE in the superior, inferior and nasal areas (ONL loss: 0–6%), however, a slight decrease was noted 36 weeks after LE (ONL loss: 12–19%). Changes in ONL thickness in the temporal quadrant were more subtle with a 3% and 6% loss (from baseline values) at respectively 2 and 36 weeks post LE. The right retina, also exposed once to the low dose, showed the same pattern of limited ONL thinning from baseline (pre-LE) after 2 weeks (Fig. 5A).

Two weeks after a single exposure to a moderate dose of white light, the *RHO*$^{T4R/T4R}$ mutant retina showed an obvious decrease in ONL thickness along the superior and temporal meridians. ONL thinning along the inferior and nasal meridians was less severe. However, thinning progressed with time, becoming much more evident at 36 weeks post LE in the inferior retina. Unexpectedly, 2 weeks after LE, the right retina (exposed at 50 weeks of age) presented a different response compared to the left retina (exposed at 16 weeks of age) that had a more severe decrease in ONL thickness along the superior and nasal meridians. While an age-related increase in resistance to light-induced damage cannot be excluded, this observation made in a single animal precludes drawing any firm conclusions.

After a single high dose of light the *RHO*$^{T4R/T4R}$ retina (OU) was severely damaged as early as 2 weeks after LE. All four meridians presented a major thinning of the ONL that expanded all along the 30° eccentricity from the edge of the ONH. At 36 weeks after LE the ONL was barely detectable in all four meridians (Figs. 5C).

No changes in ONL thickness were observed along the four meridians from any of the normal dogs after 1, 2 or 3 high dose LE (Figs. 5D).

Histologic assessment of retinal integrity was done by counting the rows of ONL nuclei from homozygous (*RHO*$^{T4R/T4R}$) mutant retinas exposed to low (Fig. 6A), moderate (Fig. 6B) and high (Fig. 6C) doses of white light. As the 30° OCT B-scans were performed only in the central retina, histological sections enabled to extend the analysis and measurements of ONL thickness to the ora serrata. This analysis confirmed the OCT imaging results by showing that the structure of the retina was severely degenerated centrally, and damage extended to the mid-periphery in eyes exposed to moderate and high doses of light. Yet, with both doses, the retinal structure was preserved in the periphery. Similarly, heterozygous (*RHO*$^{T4R/+}$) dogs that express ~ 50% mutant rhodopsin showed higher susceptibility to light damage (moderate dose) in the central and mid-peripheral superior/tapetal retina than in the inferior/non-tapetal fundus. ONL thinning in both the superior and inferior retina was more severe in dogs terminated at 6 weeks post LE, than at 2 weeks post LE (Fig 7). These results confirm the ongoing progression of photoreceptor loss several weeks after the acute insult.

3.4 The central retina in RHO$^{T4R/T4R}$ dogs is severely damaged following exposure to moderate and high doses of light

Thirty-six weeks after the exposure to the low dose of light, the morphology of the photoreceptors of the *RHO*$^{T4R/T4R}$ retina was normal (Fig. 8 A_1, A_2, A_3), and comparable to that of a WT retina exposed multiple times to the high dose of light (Fig. 8 D_1, D_2, D_3), with structurally preserved inner (IS) and outer (OS) segments apposed to the underlying RPE.

However, we did observe that the vitreal border of the ONL was irregular, possibly a result of mild photoreceptor cell loss, and subsequent ONL remodeling. As observed by *in vivo* imaging, the retinal morphology in the central/tapetal region (~ 2,000 μm from the optic disc) of $RHO^{T4R/T4R}$ retinas exposed to either moderate or high doses of light showed both a severe loss of photoreceptors and a degenerated RPE layer. Similarly, the central/non-tapetal region of eyes exposed to the high dose of light showed comparable structural alterations. IHC revealed both in the central tapetal and non-tapetal regions areas where remaining cells in the ONL were primarily cones, but these were severely altered in morphology and lacked inner and outer segments (Fig. 8 B_1–C_3).

3.5 Areas of structurally preserved photoreceptors are retained in some areas of light-exposed $RHO^{T4R/T4R}$ retinas

Amidst the central/temporal areas where retinal degeneration caused a loss of ONL, “islands” of thinner yet retained ONL could be detected by *in vivo* imaging in dogs exposed to the moderate and high doses of light. In the dog that received the high dose of light an area of ONL retention was found at ~21° from the optic nerve head (Fig. 9 A, B). Histology confirmed the retention of a thicker ONL, and fluorescence IHC showed that it was composed of rods and cones that retained, albeit disorganized, IS and OS. Within this region of retained photoreceptors was a localized area where the ONL was composed of multiple layer cone somatas (Fig. 9 D, E), a histological feature of the recently discovered cone-enriched fovea-like area.(43) The OS maintained contact with the RPE, however, this RPE was multilayered in some areas, suggesting proliferation of this retinal cell population (Fig. 9 C, D, E). No such “islands” of ONL retention were observed in the dog exposed to the low dose as the degeneration was minimal.

In vivo imaging of the peripheral retina from eyes exposed to the high dose of light showed a clear demarcation between altered and preserved ONL (Fig. 10 A, B). This was confirmed by histology/IHC which showed a clear demarcation with complete loss of PRs on the central side and a preserved ONL with intact rods and cones on the peripheral side (Fig. 10 C_1, C_2, D_1, D_2).

4. Discussion

Evidence from studies in animal models of RP that physiological levels of light exposure may influence the natural history of photoreceptor and RPE loss provide an opportunity to better understand how the interaction of a genetic defect and an environmental factor can contribute to the pathophysiology of some retinal diseases. The extreme light sensitivity in dogs that carry the naturally-occurring T4R mutation in *RHO* offers the ability to trigger in a human-sized eye an acute onset of outer retinal degeneration and examine these pathogenic mechanisms as well as responses to therapeutic intervention.(25, 39, 44, 45) In this study we demonstrate a dose-response between physiological levels of light exposure and the resulting spatio-temporal pattern of retinal degeneration. However, we do not detect in an obstacle-avoidance course any consequences of light-induced damage on visually-guided behavior.

4.1 Sensitivity of the canine T4R RHO retina to short exposures of physiological light levels

Light-induced damage of photoreceptors/RPE is dependent on several physical parameters including wavelength, intensity, duration of exposure, as well as biological factors such as animal species/strain, age, gender, degree of ocular pigmentation, body temperature, time of the circadian cycle, dark adaptation, and the contribution of specific mutations or genetic modifiers [for review see (46)]. This diversity complicates the comparison of light sensitivities between animal models as studies frequently involve the use of different light damage paradigms. However, while experimental light-induced damage in WT rodents is typically triggered by exposure to high intensity (≥ 1,100 lux) green or full spectrum white light (≥ 3,000 lux) for periods ranging from hours to days,(47–50) there is evidence for specific *RHO* mutations (P23H, S344ter, T17M, Y102H, I307N, T4R) conferring an increased sensitivity to light (for review see SI Table S1).(19, 21, 22, 24) Only few studies have investigated in these models of *RHO*-ADRP the effect of short duration light exposures. In the hT17M transgenic mouse, 2.5 minutes of illumination with 5,000 lux of white light triggers acute photoreceptor death, while limited sensitivity to a 2-fold higher intensity is found in a P23H mutant line.(19) In the Tvrm1 (Y102H) and Tvrm4 (I307N) mice, bright (12,000 lux) “achromatic” light induces retinal degeneration after an exposure of respectively 0.5 and 2 min.(21) These exposures are ~ 7.9 (19) to 3.8–15 (21) fold higher than the high dose levels used in the present study.

Studies that have investigated the light sensitivity threshold in animal models of *RHO*-ADRP are rare,(17) and thus, with the exception of the *RHO* hT17M mouse and T4R dog, it is unknown whether standard environmental illumination, or exposure to sources of light used in a clinical setting can trigger or exacerbate photoreceptor death. Fundus photography was indeed shown to be sufficient to cause acute retinal degeneration in the hT17M mouse and T4R dog, suggesting that these two models of *RHO*-ADRP are both at the high end of the spectrum of light sensitivity.(19, 25, 44, 45)

In this current study we have observed in both $RHO^{T4R/T4R}$ and $RHO^{T4R/+}$ dogs a drastic loss of ONL thickness within 2 weeks following a 1 min exposure to white light at intensities as low as 820 lux (~ corneal irradiance of 0.5 mW/cm^2). This corresponds to that of a brightly illuminated office space where common visual tasks of low contrast and small size are performed.(51) At the lowest light intensity (170 lux, ~ 0.1 mW/cm^2) no obvious thinning of the ONL could be seen at 2 weeks post exposure, but by 36 weeks mild thinning (6–19%) could be detected by OCT imaging. Depending on the retinal area, this would correspond to a loss of <1 to 2 rows of nuclei in the ONL. As the animals in this study were housed under standard kennel illuminations that ranged between 175–350 lux at the level of the dogs’ eyes, it is currently unclear whether this mild ONL thinning is the result of delayed loss of photoreceptors following acute light exposure in an eye with a dilated pupil, chronic insult from potentially phototoxic environmental levels of light, or alternatively a cell death process that is independent of light.

Dark rearing has been shown to prevent retinal degeneration in transgenic *X. laevis* expressing human P23H RHO, human T17M RHO, human N2S/N15S RHO and human T4K RHO, suggesting that activation of the degenerative process is dependent on light

exposure.(15, 16) Similar dark rearing experiments in dogs have not been performed as they would require housing the animals in darkness for > 1 year to determine if it can prevent the slow natural course of degeneration reported in T4R dogs kept under standard kennel illumination.(38) Such studies would not be approved for obvious regulatory reasons. However, housing dogs under conditions of illumination (eg. dim red light) that limit rod phototransduction may be acceptable, and the results of such a study could provide further preclinical support for assessing the benefit of light exposure restriction for some patients with class B1 RHO mutations.(12, 25)

4.2 Topographical pattern of light damage in the canine T4R RHO retina

RHO-ADRP patients with the class B1 phenotype exhibit a sectoral pattern of degeneration that affects more severely the pericentral and infero-nasal retina, than the supero-temporal retina.(11) This altitudinal defect has been associated in some clinical reports with a history of occupational exposure to bright sunlight,(13, 14) and led to recommendation that patients wear protective hats and sunglasses.(12) Whether these measures prevent or slow the progression of disease in these patients is still to be determined.

A similar predilection for disease in the inferior retina has been observed in P23H transgenic mice and *X. laevis* housed under cyclic overhead lighting,(18, 52) However, in the P23H (lines 2 and 3) and S334ter (lines 4 and 9) transgenic rats,(23) lower susceptibility of the inferior retina to acute light damage was attributed to the beneficial effect of preconditioning under dim cyclic illumination.(53) While a similar protective effect cannot be fully excluded to account for the reduced damage in the inferior region of the canine $RHO^{T4R/T4R}$ retina, (39) the asymmetry in photoreceptor loss is likely caused by the presence of a tapetum in the superior fundus. This multi-layered cellular choroidal structure (54) located behind the non-pigmented RPE is thought to play the role of a biological reflector system (55) to enhance the probability of photon capture.(56) The mutant retina that was exposed for 1 min to the moderate light intensity (820 lux; ~ corneal irradiance of 0.5 mW/cm^2) presented a clear difference in the degree of ONL loss measured by OCT between the tapetal (superior and temporal meridians) and the non-tapetal (inferior and nasal meridians) regions. However, because retinal degeneration occurred in both regions, it can be inferred that this dose of light was, even for the non-tapetal area, above the threshold for light damage.

4.3 Light damage in the canine T4R RHO retina causes acute cell death followed by a phase of chronic photoreceptor cell loss

Exposure to a similar high dose of white light (corneal irradiance of 1 mW/cm^2 for 1 min) as used in this current study has been recently shown to cause disruption of rod OS discs within minutes, and trigger a wave of synchronized photoreceptor cell death within 24 hrs.(39) In the present study, we now show that this phototoxicity results in severe outer retinal degeneration by 2 weeks post exposure in both the tapetal and non-tapetal central retina, similar to that observed following fundus photography.(25, 45) A lower dose of light (corneal irradiance of 0.5 mW/cm^2 for 1 min) caused a more moderate loss of ONL thickness at 2 weeks post exposure, but further thinning was seen at the 36 week time-point (Fig 4E2–F2, Fig 4B). These preliminary findings suggest that not all photoreceptors die

simultaneously but that a delayed and protracted loss of cells occurs for weeks after the acute insult.

This second wave of cell death may include cells that initiated repair mechanisms for survival following acute light exposure,(25, 53) but were unable to recover. In our experimental design, dogs were kept under dim red illumination for 24 hrs post light exposure to allow sufficient time for the pupils that were pharmacologically dilated for the light exposure procedure, to return to their resting state. After 24 hrs the dogs were returned to standard kennel cyclic illumination (12 hrs light at~175- 350 lux and 12 hours of dark). Based on the reported regrowth of rod OS and improved rod ERG function in P23H-3 rats maintained for 2–5 weeks under scotopic conditions following light damage,(53, 57) it is possible that in the T4R *RHO* dogs, rods that were damaged but survived the initial acute light exposure were unable to reform normal OS and subsequently died. Future studies will examine whether prolonged housing under scotopic conditions after light exposure improves repair mechanisms in this model.

Another possibility to account for this delayed loss of photoreceptors is cell death via a bystander effect, and some of the proposed mechanisms involve lack of structural support, loss of trophic support, and oxygen toxicity.(58) Alternatively, a contributing factor to the second wave of cell death is the death of RPE cells in the damaged regions. As the RPE is needed for photoreceptor maintenance and viability, loss of these cells could contribute to the progressive loss of rods, as well as cone loss; although cones do not have the opsin mutation, they too depend on the RPE for function and viability. The extended period of time (weeks) during which secondary chronic photoreceptor loss occurs following light exposure may provide a wider time window for therapeutic intervention particularly in those animal models,(50) and patients with *RHO* mutations that have a more moderate susceptibility to light.

4.4 Severe light-induced retinal damage does not alter visual behavior

Apparatus used to objectively evaluate visually-guided behavior in dogs include obstacle-avoidance courses, forced-choice mazes, and touch screen devices.(37, 40, 59, 60) These methods have been invaluable to demonstrate both the early visual impairment,(40, 59) and subsequent vision restoration following corrective gene therapy in several canine models of inherited degeneration. (34, 36, 37, 61) However, they lack precision as they test global visual function that do not evaluate visual acuity, nor test specific retinal regions for functional defects.

In this study, despite the severe loss of photoreceptors observed in the central/mid-peripheral retina, $RHO^{T4R/T4R}$ dogs retained sufficient visual function to navigate normally through an obstacle avoidance course under scotopic, mesopic, and low photopic ambient illuminations. This suggested the persistence of rods and cones able to support this visual task. OCT imaging of the far mid-peripheral retina showed an abrupt transition in ONL thickness, and histology/IHC confirmed the retention of a normal retina with rods and cones that could enable sufficient visual function for performance under the testing conditions used. This lack of pan-retinal damage could be due to topographical variation in light sensitivity across the retinal surface, alternatively it may be caused by non-uniform retinal illumination with the

hand-held monocular Ganzfeld that was used in this study. Surprisingly, an “island” of thicker, albeit abnormal ONL, was also found in the central supero-temporal quadrant of the eyes of the dog exposed to the highest dose of light. Its location corresponded to that of the recently discovered fovea-like region of the canine retina that harbors a densely packed “bouquet” of cones.(43) Immunolabeling confirmed the presence of multiple (2–3) layers of cone somatas, a characteristic feature of that area. Although distorted, surviving rods and cones at that site retained shortened IS and remnants of OS that may explain, as well, the persistence of vision under mesopic and photopic illumination. A recent study in mice has indeed demonstrated that photoreceptors lacking fully formed outer segments cause decreased visual acuity but can still support visually-guided behavior.(62)

In summary, we have confirmed the extreme light sensitivity that the T4R *RHO* mutation confers to the canine retina, and have now further refined the light damage paradigm in this model. Future studies will investigate new psychophysical tests in dogs to detect the level of visual impairment caused by this light-induced acute and progressive photoreceptor loss.

Supplementary Material

Refer to Web version on PubMed Central for supplementary material.

Acknowledgments

Svetlana Savina for histology support; Kendra McDaid for help with the visual behavior testing; Wei Pan for statistical analysis, the staff at the RDSF for animal care support, Mary Leonard for graphic support, and Drs. C. Craft and TM Redmond for providing respectively the LUMIJ and anti-RPE65 antibodies.

Supported by NIH/NEI R24EY022012, R24EY023937, 5PN2EY018241, EY06855, EY17549, P30EY-001583, Foundation Fighting Blindness, Hope for Vision and Van Sloun Fund for Canine Genetic Research.

References

1. Boughman JA, Conneally PM, Nance WE. Population genetic studies of retinitis pigmentosa. Am J Hum Genet. 1980; 32(2):223–235. [PubMed: 7386458]
2. Bunker CH, Berson EL, Bromley WC, Hayes RP, Roderick TH. Prevalence of retinitis pigmentosa in Maine. Am J Ophthalmol. 1984; 97(3):357–365. [PubMed: 6702974]
3. Hartong DT, Berson EL, Dryja TP. Retinitis pigmentosa. Lancet. 2006; 368(9549):1795–1809. [PubMed: 17113430]
4. Sung CH, Davenport CM, Hennessey JC, Maumenee IH, Jacobson SG, Heckenlively JR, et al. Rhodopsin mutations in autosomal dominant retinitis pigmentosa. Proc Natl Acad Sci U S A. 1991; 88(15):6481–6485. [PubMed: 1862076]
5. Inglehearn CF, Keen TJ, Bashir R, Jay M, Fitzke F, Bird AC, et al. A completed screen for mutations of the rhodopsin gene in a panel of patients with autosomal dominant retinitis pigmentosa. Hum Mol Genet. 1992; 1(1):41–45. [PubMed: 1301135]
6. Sohocki MM, Daiger SP, Bowne SJ, Rodriquez JA, Northrup H, Heckenlively JR, et al. Prevalence of mutations causing retinitis pigmentosa and other inherited retinopathies. Hum Mutat. 2001; 17(1):42–451. [PubMed: 11139241]
7. Sullivan LS, Bowne SJ, Birch DG, Hughbanks-Wheaton D, Heckenlively JR, Lewis RA, et al. Prevalence of disease-causing mutations in families with autosomal dominant retinitis pigmentosa: a screen of known genes in 200 families. Invest Ophthalmol Vis Sci. 2006; 47(7):3052–3064. [PubMed: 16799052]

8. Audo I, Manes G, Mohand-Said S, Friedrich A, Lancelot ME, Antonio A, et al. Spectrum of rhodopsin mutations in French autosomal dominant rod-cone dystrophy patients. Invest Ophthalmol Vis Sci. 2010; 51(7):3687–3700. [PubMed: 20164459]
9. Sullivan LS, Bowne SJ, Reeves MJ, Blain D, Goetz K, Ndifor V, et al. Prevalence of Mutations in eyeGENE Probands With a Diagnosis of Autosomal Dominant Retinitis Pigmentosa. Invest Ophthalmol Vis Sci. 2013; 54(9):6255–6261. [PubMed: 23950152]
10. Gal A, Apfelstedt-Sylla E, Janecke AR, Zrenner E. Rhodopsin mutations in inherited retinal dystrophie and dysfunctions. Prog Ret Eye Res. 1997; 16(1):51–79.
11. Cideciyan AV, Hood DC, Huang Y, Banin E, Li ZY, Stone EM, et al. Disease sequence from mutant rhodopsin allele to rod and cone photoreceptor degeneration in man. Proc Natl Acad Sci U S A. 1998; 95(12):7103–7108. [PubMed: 9618546]
12. Paskowitz DM, LaVail MM, Duncan JL. Light and inherited retinal degeneration. Br J Ophthalmol. 2006; 90(8):1060–1066. [PubMed: 16707518]
13. Heckenlively JR, Rodriguez JA, Daiger SP. Autosomal dominant sectoral retinitis pigmentosa. Two families with transversion mutation in codon 23 of rhodopsin. Arch Ophthalmol. 1991; 109(1):84–91. [PubMed: 1987955]
14. Iannaccone A, Man D, Waseem N, Jennings BJ, Ganapathiraju M, Gallaher K, et al. Retinitis pigmentosa associated with rhodopsin mutations: Correlation between phenotypic variability and molecular effects. Vision Res. 2006; 46(27):4556–4567. [PubMed: 17014888]
15. Tam BM, Moritz OL. Dark rearing rescues P23H rhodopsin-induced retinal degeneration in a transgenic Xenopus laevis model of retinitis pigmentosa: a chromophore-dependent mechanism characterized by production of N-terminally truncated mutant rhodopsin. J Neurosci. 2007; 27(34):9043–9053. [PubMed: 17715341]
16. Tam BM, Moritz OL. The role of rhodopsin glycosylation in protein folding, trafficking, and light-sensitive retinal degeneration. J Neurosci. 2009; 29(48):15145–15154. [PubMed: 19955366]
17. Tam BM, Qazalbash A, Lee HC, Moritz OL. The dependence of retinal degeneration caused by the rhodopsin P23H mutation on light exposure and vitamin a deprivation. Invest Ophthalmol Vis Sci. 2010; 51(3):1327–1334. [PubMed: 19933196]
18. Naash ML, Peachey NS, Li ZY, Gryczan CC, Goto Y, Blanks J, et al. Light-induced acceleration of photoreceptor degeneration in transgenic mice expressing mutant rhodopsin. Invest Ophthalmol Vis Sci. 1996; 37(5):775–782. [PubMed: 8603862]
19. White DA, Fritz JJ, Hauswirth WW, Kaushal S, Lewin AS. Increased sensitivity to light-induced damage in a mouse model of autosomal dominant retinal disease. Invest Ophthalmol Vis Sci. 2007; 48(5):1942–1951. [PubMed: 17460245]
20. Krebs MP, White DA, Kaushal S. Biphasic photoreceptor degeneration induced by light in a T17M rhodopsin mouse model of cone bystander damage. Invest Ophthalmol Vis Sci. 2009; 50(6):2956–2965. [PubMed: 19136713]
21. Budzynski E, Gross AK, McAlear SD, Peachey NS, Shukla M, He F, et al. Mutations of the opsin gene (Y102H and I307N) lead to light-induced degeneration of photoreceptors and constitutive activation of phototransduction in mice. J Biol Chem. 2010; 285(19):14521–14533. [PubMed: 20207741]
22. Organisciak DT, Darrow RM, Barsalou L, Kutty RK, Wiggert B. Susceptibility to retinal light damage in transgenic rats with rhodopsin mutations. Invest Ophthalmol Vis Sci. 2003; 44(2):486–492. [PubMed: 12556372]
23. Vaughan DK, Coulibaly SF, Darrow RM, Organisciak DT. A morphometric study of light-induced damage in transgenic rat models of retinitis pigmentosa. Invest Ophthalmol Vis Sci. 2003; 44(2):848–855. [PubMed: 12556421]
24. Walsh N, van Driel D, Lee D, Stone J. Multiple vulnerability of photoreceptors to mesopic ambient light in the P23H transgenic rat. Brain Res. 2004; 1013(2):194–203. [PubMed: 15193529]
25. Cideciyan AV, Jacobson SG, Aleman TS, Gu D, Pearce-Kelling SE, Sumaroka A, et al. In vivo dynamics of retinal injury and repair in the rhodopsin mutant dog model of human retinitis pigmentosa. Proc Natl Acad Sci U S A. 2005; 102(14):5233–5238. [PubMed: 15784735]

26. Mendes HF, van der Spuy J, Chapple JP, Cheetham ME. Mechanisms of cell death in rhodopsin retinitis pigmentosa: implications for therapy. Trends Mol Med. 2005; 11(4):177–185. [PubMed: 15823756]
27. Mendes HF, Cheetham ME. Pharmacological manipulation of gain-of-function and dominant-negative mechanisms in rhodopsin retinitis pigmentosa. Hum Mol Genet. 2008; 17(19):3043–3054. [PubMed: 18635576]
28. Saliba RS, Munro PM, Luthert PJ, Cheetham ME. The cellular fate of mutant rhodopsin: quality control, degradation and aggresome formation. J Cell Sci. 2002; 115(Pt 14):2907–2918. [PubMed: 12082151]
29. Rajan RS, Kopito RR. Suppression of wild-type rhodopsin maturation by mutants linked to autosomal dominant retinitis pigmentosa. J Biol Chem. 2005; 280(2):1284–1291. [PubMed: 15509574]
30. Mao H, Thomas J, Schewein A, Shabashvili A, Hauswirth WW, Gorbatyuk MS, et al. AAV Delivery of Wild-Type Rhodopsin Preserves Retinal Function in a Mouse Model of Autosomal Dominant Retinitis Pigmentosa. Hum Gene Ther. 2011; 22(5):567–575. [PubMed: 21126223]
31. Mao H, Gorbatyuk MS, Rossmiller B, Hauswirth WW, Lewin AS. Long-term rescue of retinal structure and function by rhodopsin RNA replacement with a single adeno-associated viral vector in P23H RHO transgenic mice. Hum Gene Ther. 2012; 23(4):356–366. [PubMed: 22289036]
32. Millington-Ward S, Chadderton N, O'Reilly M, Palfi A, Goldmann T, Kilty C, et al. Suppression and Replacement Gene Therapy for Autosomal Dominant Disease in a Murine Model of Dominant Retinitis Pigmentosa. Mol Ther. 2011; 19(4):642–649. [PubMed: 21224835]
33. Acland GM, Aguirre GD, Ray J, Zhang Q, Aleman TS, Cideciyan AV, et al. Gene therapy restores vision in a canine model of childhood blindness. Nat Genet. 2001; 28(1):92–95. [PubMed: 11326284]
34. Komaromy AM, Alexander JJ, Rowlan JS, Garcia MM, Chiodo VA, Kaya A, et al. Gene therapy rescues cone function in congenital achromatopsia. Hum Mol Genet. 2010; 19(13):2581–2593. [PubMed: 20378608]
35. Petit L, Lheriteau E, Weber M, Le Meur G, Deschamps JY, Provost N, et al. Restoration of vision in the pde6beta-deficient dog, a large animal model of rod-cone dystrophy. Mol Ther. 2012; 20(11):2019–2030. [PubMed: 22828504]
36. Lheriteau E, Petit L, Weber M, Le Meur G, Deschamps JY, Libeau L, et al. Successful gene therapy in the RPGRIP1-deficient dog: a large model of cone-rod dystrophy. Mol Ther. 2013; 22(2):265–277. [PubMed: 24091916]
37. Beltran WA, Cideciyan AV, Iwabe S, Swider M, Kosyk MS, McDaid K, et al. Successful arrest of photoreceptor and vision loss expands the therapeutic window of retinal gene therapy to later stages of disease. Proc Natl Acad Sci U S A. 2015; 112(43):E5844–E5853. [PubMed: 26460017]
38. Kijas JW, Cideciyan AV, Aleman TS, Pianta MJ, Pearce-Kelling SE, Miller BJ, et al. Naturally occurring rhodopsin mutation in the dog causes retinal dysfunction and degeneration mimicking human dominant retinitis pigmentosa. Proc Natl Acad Sci U S A. 2002; 99(9):6328–6333. [PubMed: 11972042]
39. Marsili S, Genini S, Sudharsan R, Gingrich J, Aguirre GD, Beltran WA. Exclusion of the Unfolded Protein Response in Light-Induced Retinal Degeneration in the Canine T4R RHO Model of Autosomal Dominant Retinitis Pigmentosa. PLoS ONE. 2015; 10(2):e0115723. [PubMed: 25695253]
40. Garcia MM, Ying GS, Cocores CA, Tanaka JC, Komaromy AM. Evaluation of a behavioral method for objective vision testing and identification of achromatopsia in dogs. Am J Vet Res. 2010; 71(1):97–102. [PubMed: 20043788]
41. Beltran WA, Hammond P, Acland GM, Aguirre GD. A frameshift mutation in *RPGR* exon ORF15 causes photoreceptor degeneration and inner retina remodeling in a model of X-linked retinitis pigmentosa. Invest Ophthalmol Vis Sci. 2006; 47(4):1669–1681. [PubMed: 16565408]
42. Liang K-Y, Zeger SL. Longitudinal analysis using generalized linear models. Biometrika. 1986; 73(1):13–22.

43. Beltran WA, Cideciyan AV, Guziewicz KE, Iwabe S, Swider M, Scott EM, et al. Canine retina has a primate fovea-like bouquet of cone photoreceptors which is affected by inherited macular degenerations. PLoS ONE. 2014; 9(3):e90390. [PubMed: 24599007]
44. Gu D, Beltran WA, Li Z, Acland GM, Aguirre GD. Clinical light exposure, photoreceptor degeneration, and AP-1 activation: a cell death or cell survival signal in the rhodopsin mutant retina? Invest Ophthalmol Vis Sci. 2007; 48(11):4907–4918. [PubMed: 17962438]
45. Gu D, Beltran WA, Pearce-Kelling S, Li Z, Acland GM, Aguirre GD. Steroids do not prevent photoreceptor degeneration in the light-exposed T4R rhodopsin mutant dog retina irrespective of AP-1 inhibition. Invest Ophthalmol Vis Sci. 2009; 50(7):3482–3494. [PubMed: 19234347]
46. De Vera Mudry MC, Kronenberg S, Komatsu S, Aguirre GD. Blinded by the light: retinal phototoxicity in the context of safety studies. Toxicol Pathol. 2013; 41(6):813–825. [PubMed: 23271306]
47. Noell WK, Walker VS, Kang BS, Berman S. Retinal damage by light in rats. Invest Ophthalmol. 1966; 5(5):450–473. [PubMed: 5929286]
48. Tanito M, Kaidzu S, Ohira A, Anderson RE. Topography of retinal damage in light-exposed albino rats. Exp Eye Res. 2008; 87(3):292–295. [PubMed: 18586030]
49. Organisciak DT, Vaughan DK. Retinal light damage: mechanisms and protection. Prog Retin Eye Res. 2010; 29(2):113–134. [PubMed: 19951742]
50. Montalban-Soler L, Alarcon-Martinez L, Jimenez-Lopez M, Salinas-Navarro M, Galindo-Romero C, Bezerra de Sa F, et al. Retinal compensatory changes after light damage in albino mice. Mol Vis. 2012; 18:675–693. [PubMed: 22509098]
51. America IESoN. IESNA Lighting handbook (9th). 2000
52. Zhang R, Oglesby E, Marsh-Armstrong N. Xenopus laevis P23H rhodopsin transgene causes rod photoreceptor degeneration that is more severe in the ventral retina and is modulated by light. Exp Eye Res. 2008; 86(4):612–621. [PubMed: 18291367]
53. Chrysostomou V, Stone J, Stowe S, Barnett NL, Valter K. The status of cones in the rhodopsin mutant P23H-3 retina: light-regulated damage and repair in parallel with rods. Invest Ophthalmol Vis Sci. 2008; 49(3):1116–1125. [PubMed: 18326739]
54. Lesiuk TP, Braekevelt CR. Fine structure of the canine tapetum lucidum. Journal of anatomy. 1983; 136(Pt 1):157–164. [PubMed: 6833116]
55. Weale RA. The spectral reflectivity of the cat's tapetum measured in situ. The Journal of physiology. 1953; 119(1):30–42. [PubMed: 13035715]
56. Ollivier FJ, Samuelson DA, Brooks DE, Lewis PA, Kallberg ME, Komaromy AM. Comparative morphology of the tapetum lucidum (among selected species). Vet Ophthalmol. 2004; 7(1):11–22. [PubMed: 14738502]
57. Jozwick C, Valter K, Stone J. Reversal of functional loss in the P23H-3 rat retina by management of ambient light. Exp Eye Res. 2006; 83(5):1074–1080. [PubMed: 16822506]
58. Stone J, Maslim J, Valter-Kocsi K, Mervin K, Bowers F, Chu Y, et al. Mechanisms of photoreceptor death and survival in mammalian retina. Prog Retin Eye Res. 1999; 18(6):689–735. [PubMed: 10530749]
59. Gearhart PM, Gearhart CC, Petersen-Jones SM. A novel method for objective vision testing in canine models of inherited retinal disease. Invest Ophthalmol Vis Sci. 2008; 49(8):3568–3576. [PubMed: 18660425]
60. Muller CA, Schmitt K, Barber AL, Huber L. Dogs can discriminate emotional expressions of human faces. Curr Biol. 2015; 25(5):601–605. [PubMed: 25683806]
61. Narfstrom K, Katz ML, Ford M, Redmond TM, Rakoczy E, Bragadottir R. In vivo gene therapy in young and adult RPE65−/− dogs produces long-term visual improvement. J Hered. 2003; 94(1): 31–37. [PubMed: 12692160]
62. Thompson S, Blodi FR, Lee S, Welder CR, Mullins RF, Tucker BA, et al. Photoreceptor cells with profound structural deficits can support useful vision in mice. Invest Ophthalmol Vis Sci. 2014; 55(3):1859–1866. [PubMed: 24569582]

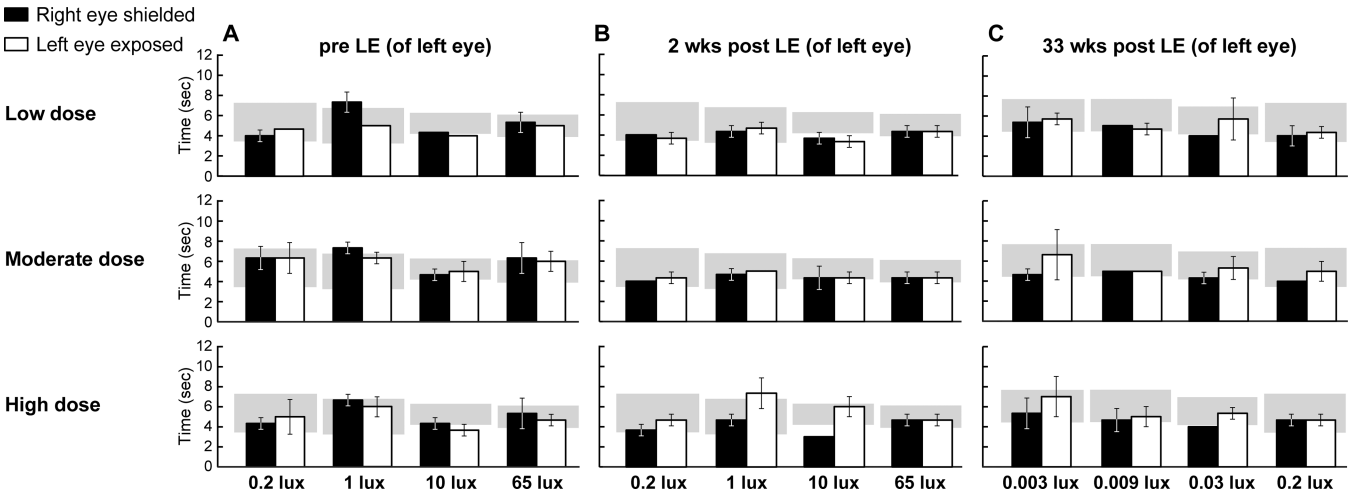

Figure 1.

Transit times of *RHO*$^{T4R/T4R}$ dogs through the obstacle-avoidance course following exposure to a low, moderate or high dose of light to the left eye. **(A)** Transit times under mesopic/photopic illuminations before light exposure (LE). **(B)** Transit times under mesopic/photopic illuminations 2 weeks post exposure. **(C)** Transit time under scotopic/mesopic illuminations 33 week post exposure. Values are: Mean ± SD of 3 runs. Grey area represents transit time (95% CI) from other WT dogs (Beltran et al. PNAS, 2015; 112: E5844-53) tested under scotopic, mesopic, and photopic illuminations. LE: light exposure.

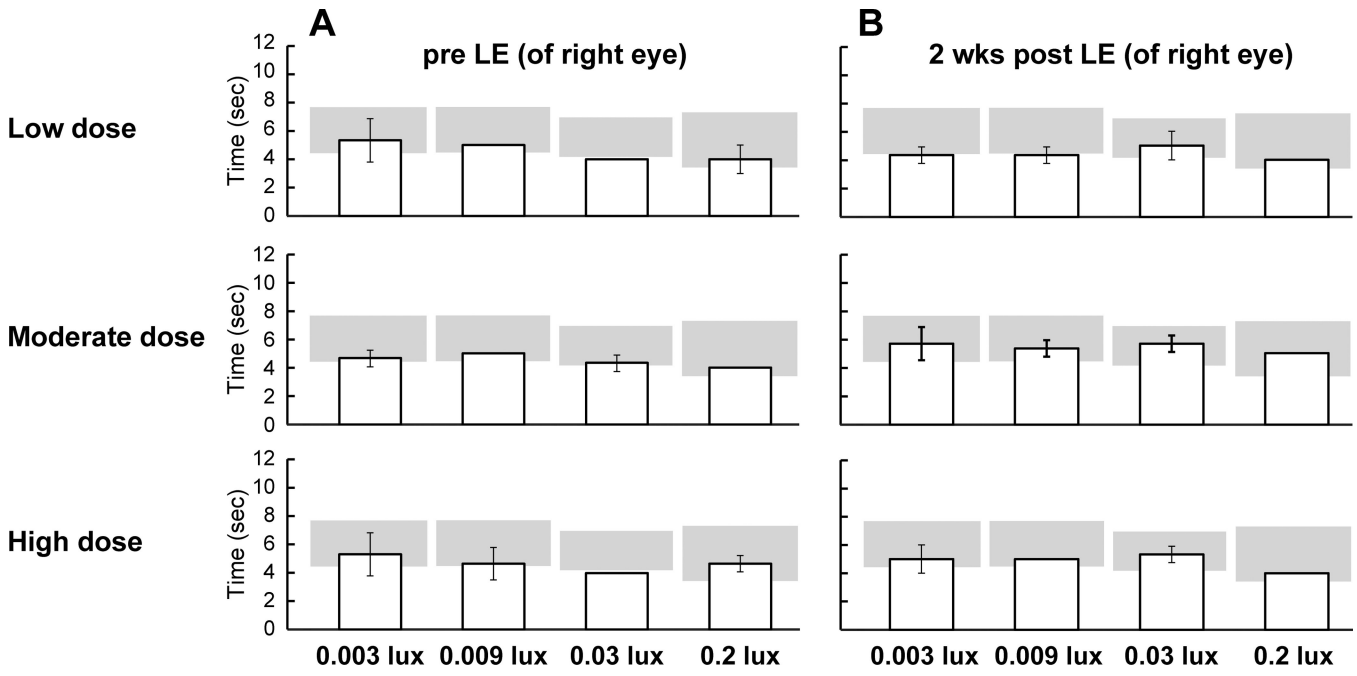

Figure 2.

Transit times of *RHO*$^{T4R/T4R}$ dogs through the obstacle-avoidance (N=3) course under scotopic/mesopic ambient illuminations after light exposure (LE) to the right eye. **(A)** Transit times 1 week before LE **(B)** Transit times 2 weeks after LE. Values are: Mean ± SD of 3 runs. Grey area represents transit time (95% CI) from other WT dogs (Beltran et al. PNAS, 2015; 112: E5844-53) tested under scotopic/mesopic illuminations; LE: light exposure.

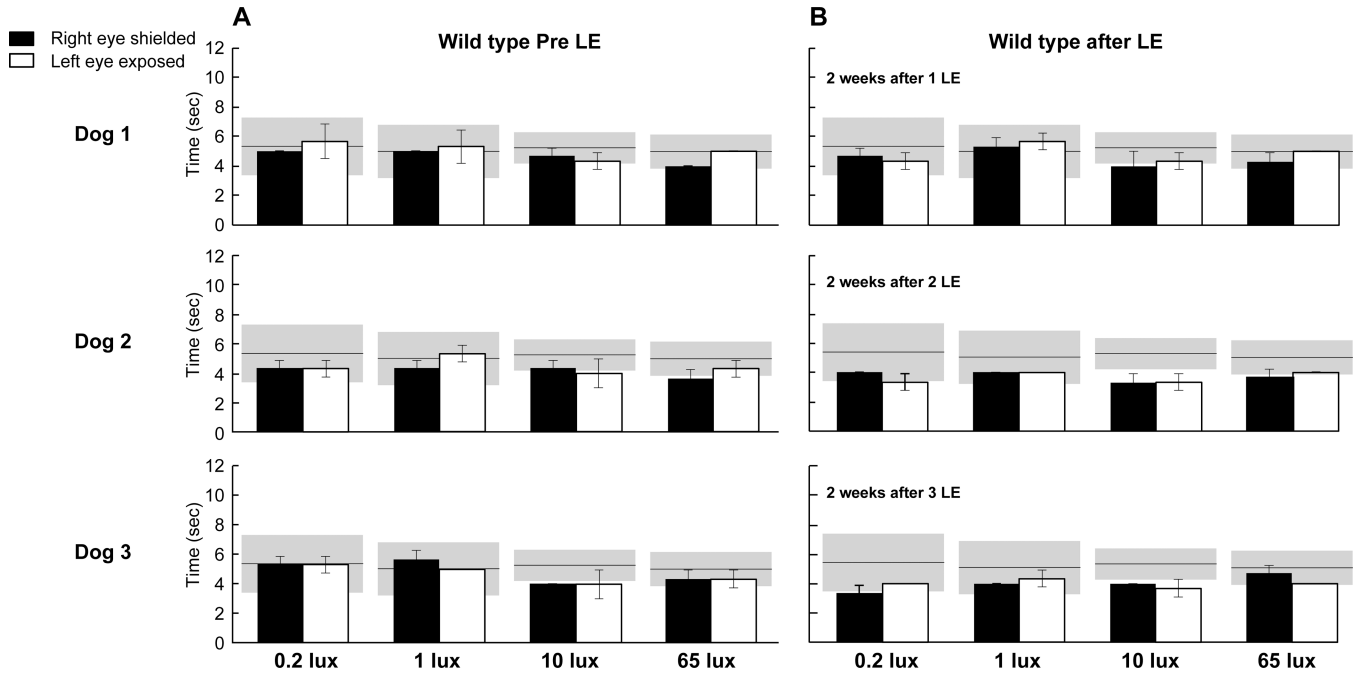

Figure 3.

Transit times of WT dogs (N=3) through the obstacle-avoidance course following one, two, or three exposures to the high dose of light in the left eye. **(A)** Transit times under mesopic/photopic illuminations before light exposure (LE). **(B)** Transit times under mesopic/photopic illuminations 2 weeks post exposure. Values are: Mean ± SD of 3 runs. Grey area represents transit time (95% CI) from other WT dogs tested under mesopic, and photopic illuminations (Beltran et al. PNAS, 2015; 112: E5844-53). LE: light exposure.

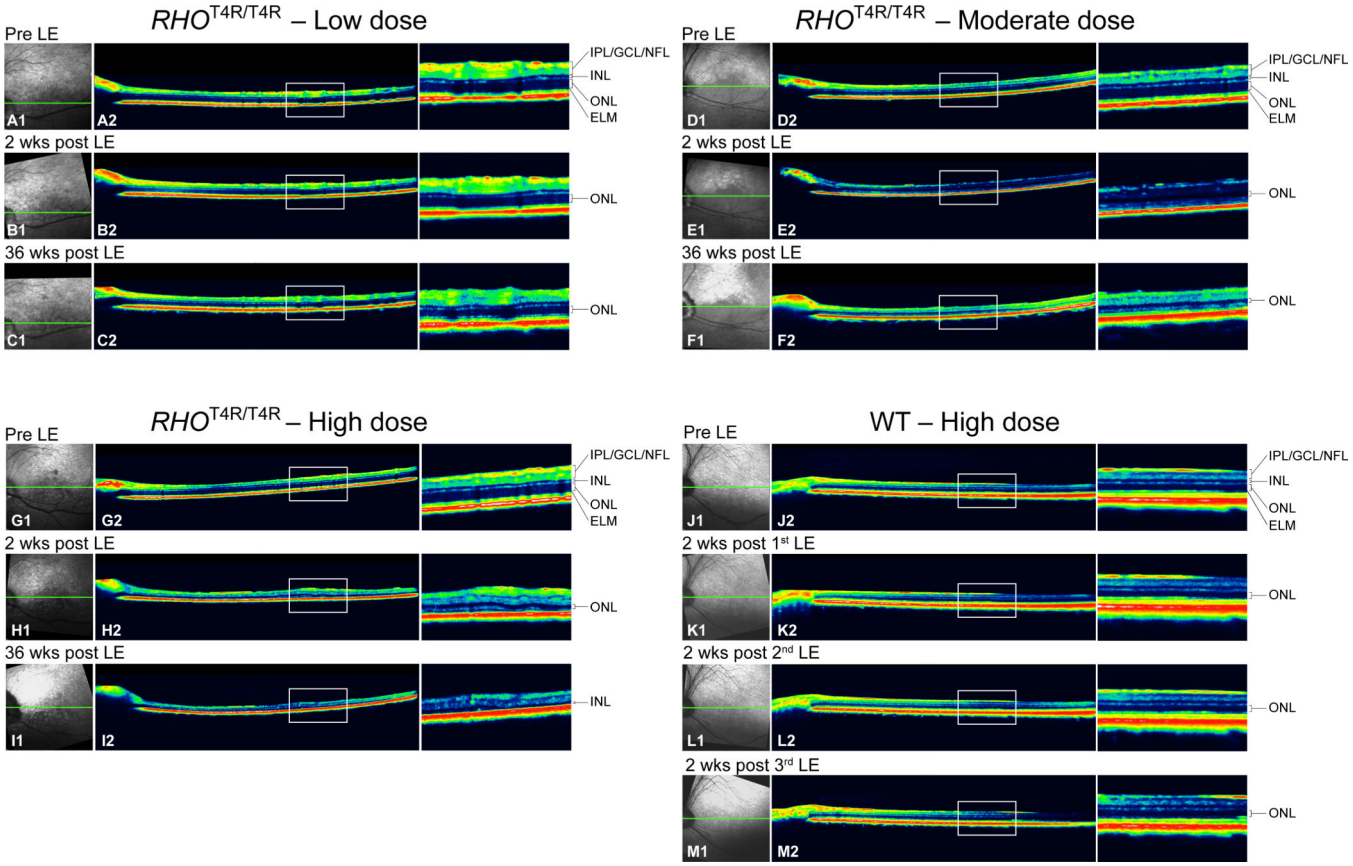

Figure 4.

cSLO/sdOCT images of the temporal area from *RHO*$^{T4R/T4R}$ and normal retinas following light exposure (LE) to different intensities of light. Confocal SLO images showed no changes in retinal vasculature in retina exposed to the low dose of light at 2 or 36 weeks after LE **(A_1, B_1, C_1)**. However retinal vasculature attenuation was noted as early as 2 weeks after exposure to moderate and high dose intensities of light **(D_1, E_1, F_1, G_1, H_1, I_1)**. No vascular changes were observed in the normal retina after 1, 2, or 3 high LE doses **(J_1, K_1, L_1, M_1)**. OCT single scans showed no changes in ONL thickness 2 weeks after exposure to the low dose **(A_2, B_2)**, yet subtle thinning was observed 36 weeks after LE **(C_2)**. Retinas exposed to either a moderate or a high dose showed a severe decrease in ONL thickness at 2 weeks after LE **(D_2, E_2, G_2, H_2)**; thinning was more evident at 36 weeks after LE **(F_2, I_2)**. The high dose did not cause any change in retinal thickness in wild type dogs after single or multiple LE **(J_2, K_2, L_2, M_2)**. Green line shows the level of the OCT B-scan; LE: light exposure.

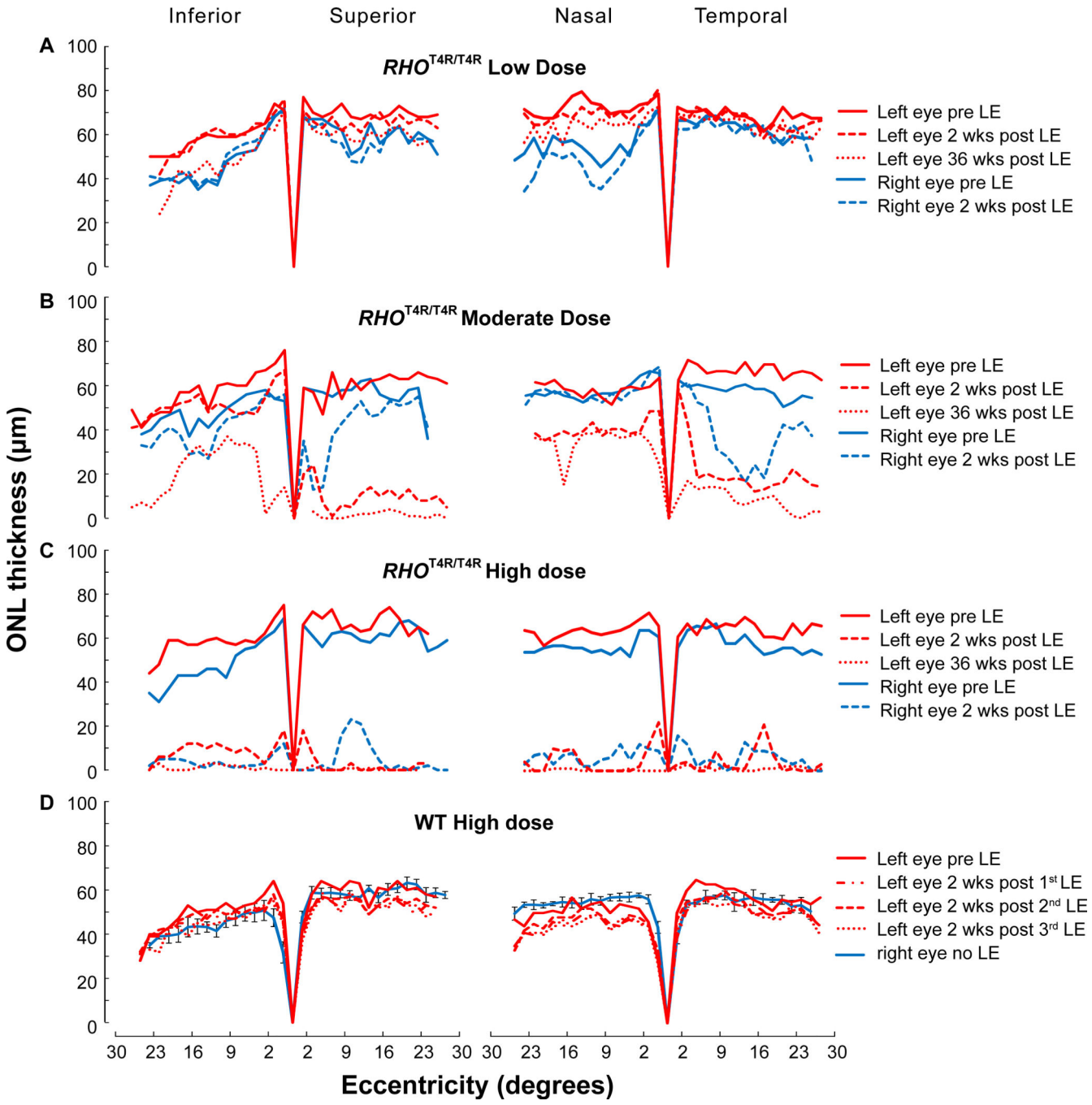

Figure 5.

Spider graphs of ONL thickness along the 4 meridians of *RHO*$^{T4R/T4R}$ and WT retinas measured by manual segmentation from sd-OCT B-scans. ONL thickness in *RHO*$^{T4R/T4R}$ retinas exposed to a low **(A)**, moderate **(B)**, and high **(C)** dose of light. **(D)** ONL thickness in WT retinas shielded (Right eye no LE; Mean± SD) or exposed (Left eye) to repeated high doses of light. LE: light exposure.

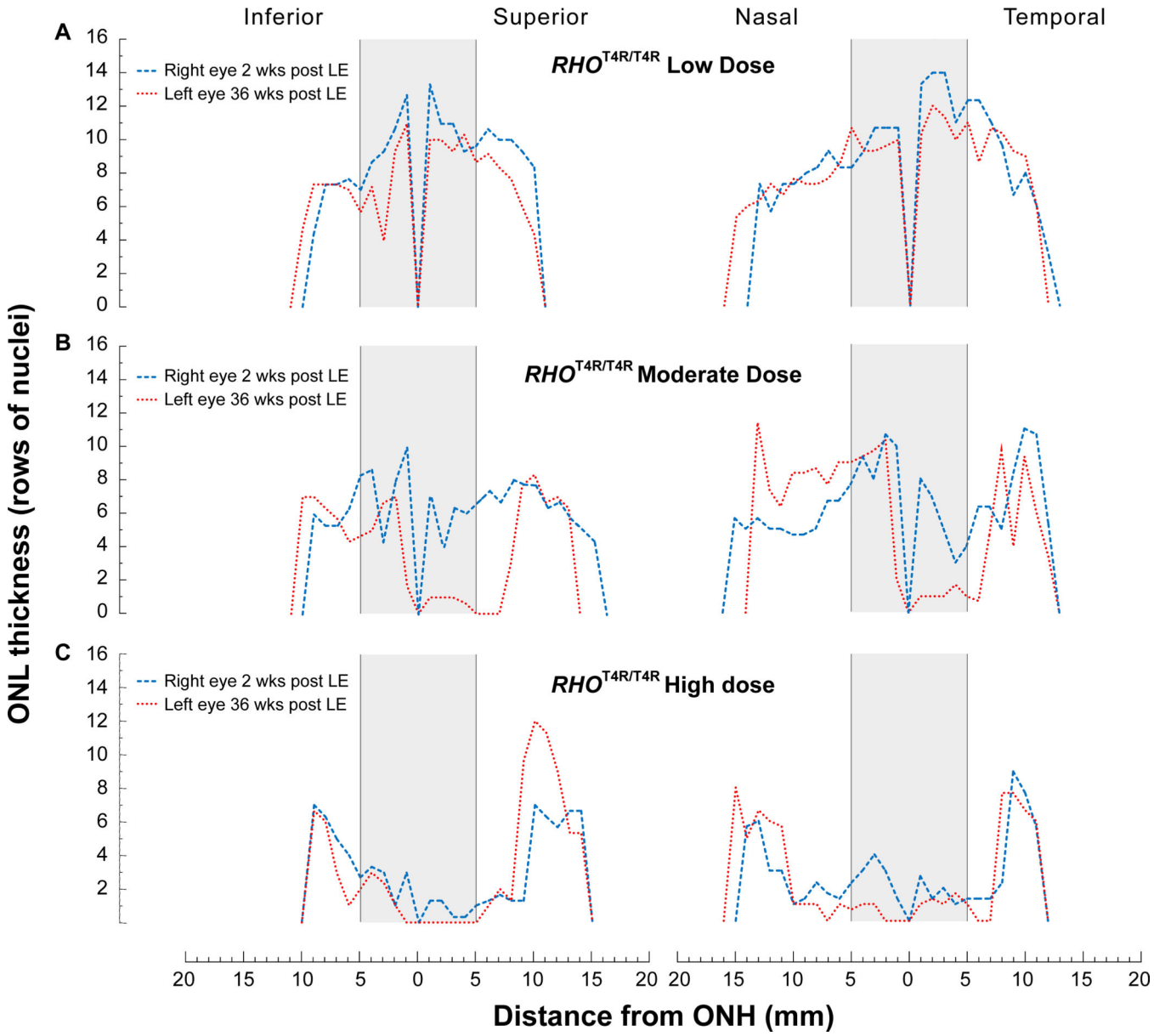

Figure 6.

Spider graphs of ONL thickness along the 4 meridians of *RHO*$^{T4R/T4R}$ retinas measured from histological sections. ONL thickness in *RHO*$^{T4R/T4R}$ retinas 2 weeks (Right eye) and 36 weeks (Left eye) after exposure to a low **(A)**, moderate **(B)**, and high **(C)** dose of light. Grey boxes illustrate the approximate central region imaged by OCT (approximate 30°) and were based on the recognition of landmarks seen in both OCT scans and H&E sections.

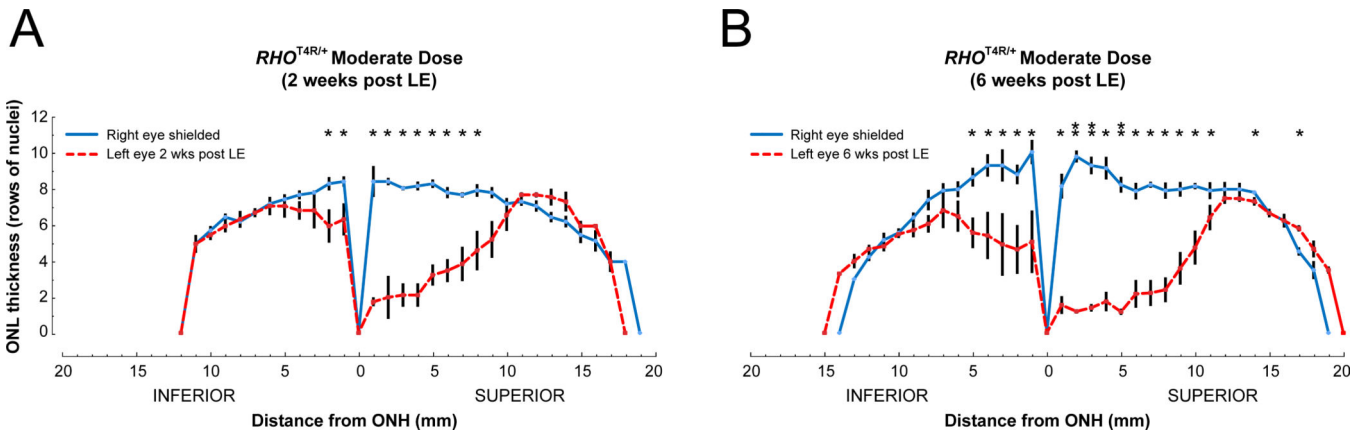

Figure 7.

Spider graphs of ONL thickness along the inferior and superior meridian of *RHO*$^{T4R/+}$retinas measured from histological sections. **(A)** ONL thickness (mean ± SEM; n = 4) before and 2 weeks after exposure to a moderate dose of light. **(B)** ONL thickness (mean ± SEM; n = 4) before and 6 weeks after exposure to a moderate dose of light. *P < 0.05; **P < 0.001; Paired Student's t test (1-tailed).

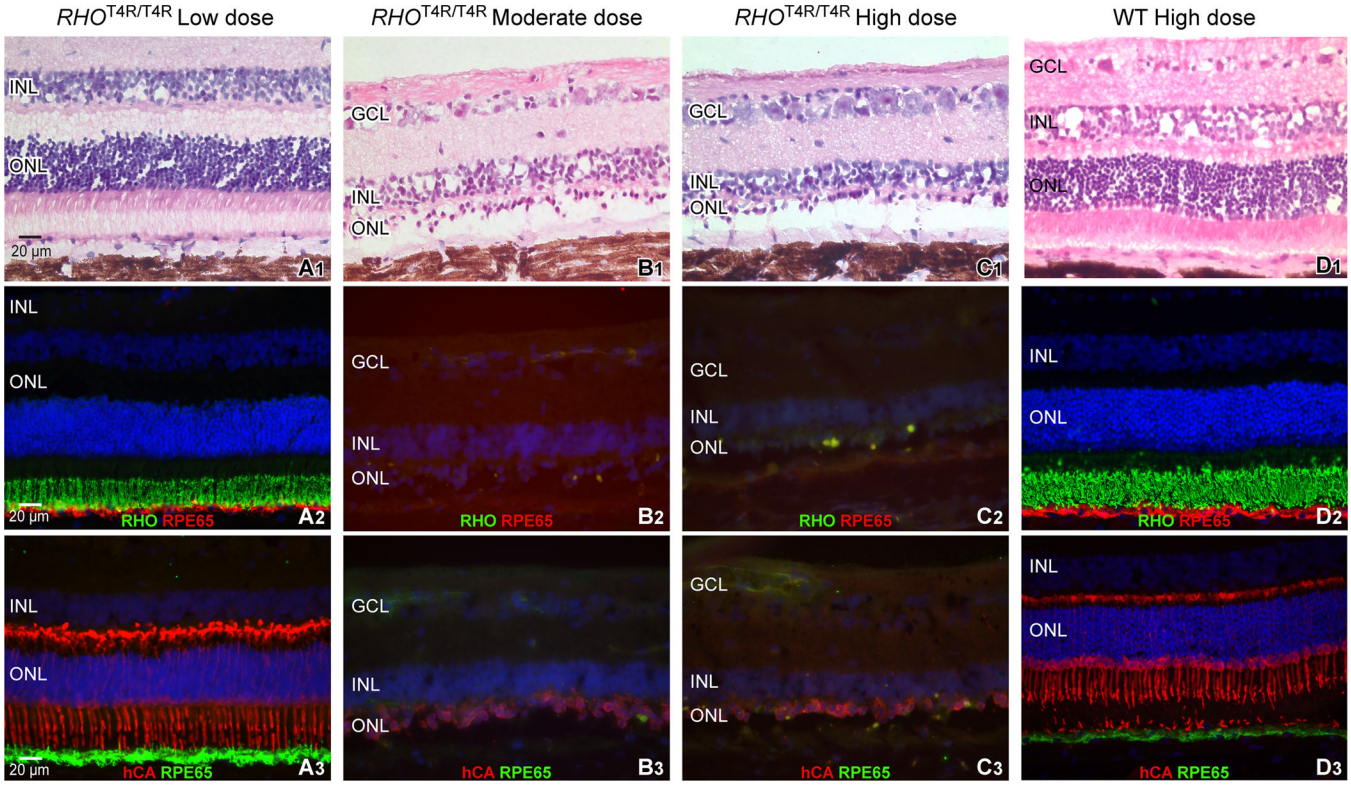

Figure 8.

Morphologic appearance of photoreceptors and retinal pigment epithelium (RPE) in the central retina of *RHO*$^{T4R/T4R}$ 36 weeks following a single exposure to a low, moderate, or high dose of light; and of WT retinas following repeated (3) light exposures to a high dose of light. Histological images were taken 2,000 µm temporal from the edge of the optic nerve head. (**A1, B1, C1, D1**): H&E stained cryosections. (**A2, B2, C2, D2**): Double fluorescence immunohistochemistry with cell-specific labeling of rod outer segments (RHO, in green) and of the retinal pigment epithelium (RPE65, in red). (**A3, B3, C3, D3**): Double fluorescence immunohistochemistry with cell-specific labeling of cones (hCA, in red) and of the retinal pigment epithelium (RPE65, in green). RGC: retinal ganglion cell layer; INL: inner nuclear layer; ONL: outer nuclear layer; RHO: rod opsin, hCA: human cone arrestin.

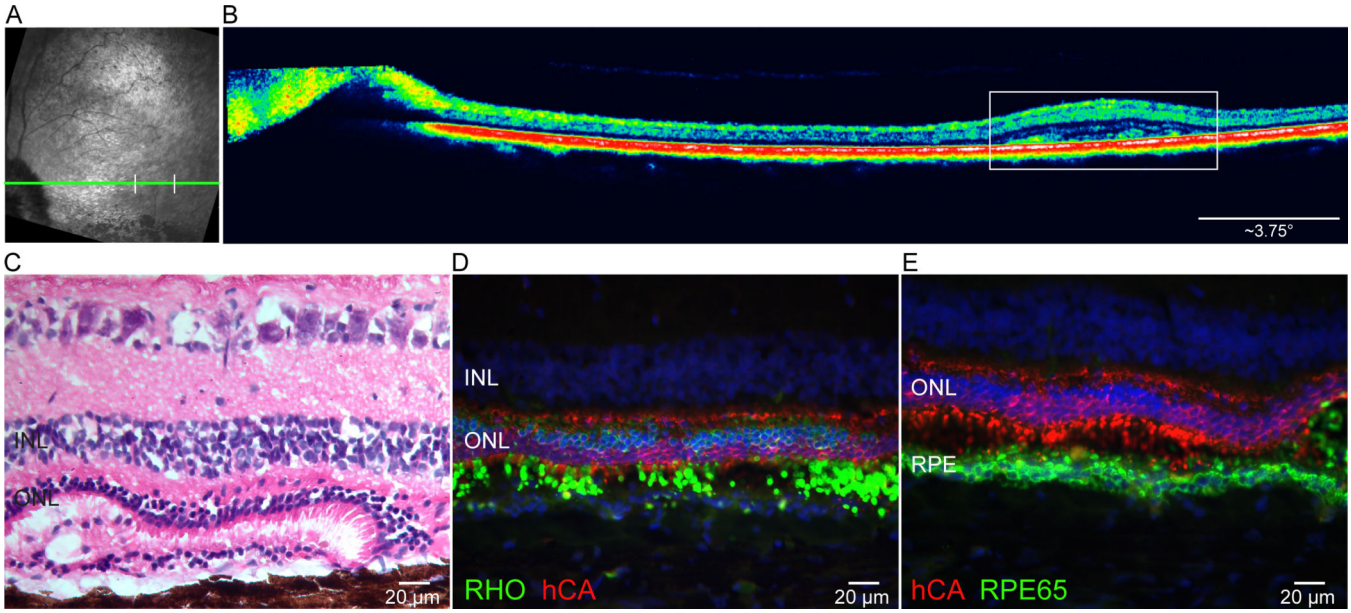

Figure 9.

In vivo imaging and histology from the *RHO*$^{T4R/T4R}$ retina exposed to the high dose showing evidence of focal areas of preserved ONL at 36 weeks post light exposure. **(A)** cSLO image from the temporal region showing retinal vasculature attenuation in the central retina. Green line indicates the level of the OCT B-scan shown in B, and white vertical bars the site of preserved ONL. **(B)** sd-OCT scan showing a small area of thicker ONL (white rectangle). **(C)** Histology section cut through the region of ONL thickening. **(D)** Double-fluorescence IHC labeling in the region of increased ONL thickness confirms the presence of an increased number of surviving rods (RHO; green) and a multiple layers of cones (hCA; red). **(E)** Double-fluorescence IHC labeling showing retention of cone outer segments (hCA; red) and a multi-layered retinal pigment epithelium (RPE65; green). INL: inner nuclear layer; ONL: outer nuclear layer.

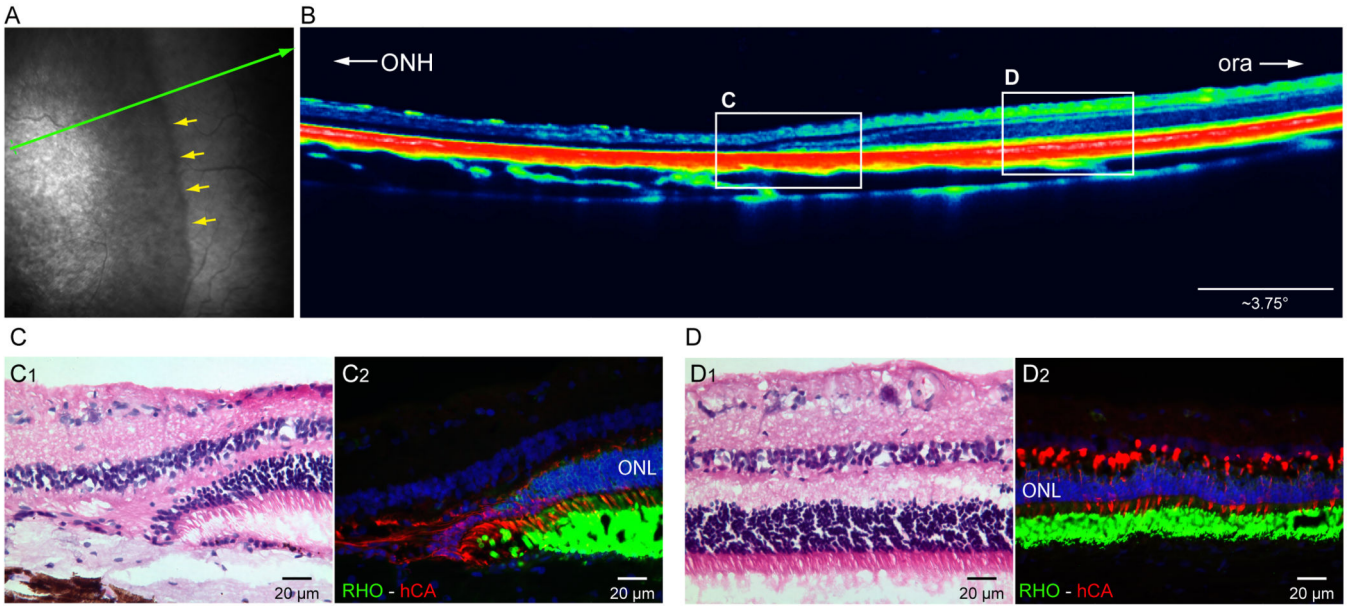

Figure 10.

Peripheral retina (up to ~ 4,000 μm from the ora serrata) of the *RHO*$^{T4R/T4R}$ is preserved from light-induced damage. **(A)** Near infrared cSLO shows a clear change in retinal reflectivity (yellow arrows) 36 weeks post exposure to a high dose of light. Green arrow shows location of OCT B-scan shown in (B). **(B)** sd-OCT B-scan shows an abrupt transition in retinal and ONL thickness with a preservation of lamination in the periphery. White rectangles indicate the approximate location of the histology images show below **(C, D)**. H&E **(C1)** and immunolabeled **(C2)** sections showing abrupt change in ONL thickness at the transition zone. **(D1)** H&E stained section showing normal retinal structure in the periphery, **(D2)** Double fluorescence IHC confirms that both rods (RHO, green), and cones (hCA, red) are spared from damage in the peripheral retina. ONH: optic nerve head; ora: ora serrata;-RHO: rod opsin; hCA: human cone arrestin. ONL: outer nuclear layer.

Table 1

Antibodies used for immunohistochemistry. (pc: polyclonal, mc: monoclonal).

Antigen	Host	Source*	Working concentrations
Rod opsin	Mouse mc	Millipore, clone RET-P1/MAB5316	1:200
Human cone arrestin	Rabbit pc	Cheryl Craft, LUMIF (University of Southern California, Los Angeles, CA	1:10,000
RPE65	Mouse pc	Novus Biologicals, NB-100-355	1:200
RPE65	Rabbit pc	Gift from T.M. Redmond NIH	1:200

*Catalog numbers for commercially available antibodies are listed as a reference to their specificity.